Inorg. Chem. **2007**, *46*, 9906–9911

Structures and Physical Properties of New Semiconducting Polyselenides $Ba_2Cu_\delta Ag_{4-\delta}Se_5$ with Unprecedented Linear Se_3^{4-} Units

Abdeljalil Assoud, Jianxiao Xu, and Holger Kleinke*

Department of Chemistry, University of Waterloo, Waterloo, Ontario, Canada N2L 3G1

Received June 28, 2007

The title compounds were prepared from the elements in evacuated silica tubes at 650 °C, followed by slow cooling. $Ba_2Ag_4Se_5$ forms a new structure type, space group *C*2/*m*, with $a = 16.189(2)$ Å, $b = 4.5528(6)$ Å, $c = 9.2500(1)$ Å, $\beta = 124.572(3)°$, and $V = 561.4(1)$ Å^3 ($Z = 2$). A maximum of 44% of the Ag atoms may be replaced with Cu atoms without changing the structure type. The crystal structure is composed of $Ag_4Se_5^{4-}$ layers, interconnected via the Ba^{2+} cations. The Ag atoms show irregular [3 + 1] coordination by the Se atoms, and the Ba atoms are located in capped square antiprisms formed by Se atoms. Most intriguing is the unprecedented occurrence of linear Se_3^{4-} units. According to the formulation $(Ba^{2+})_2(Ag^+)_4Se_3^{4-}(Se^{2-})_2$, this selenide is electron-precise with eight positive charges equalizing the eight negative charges. Electronic structure calculations indicated the presence of a band gap, as was experimentally confirmed: the electrical conductivity measurement revealed a gap of 0.6 eV for $Ba_2CuAg_3Se_5$.

Introduction

A large number of polychalcogenides exhibit various and, in part, uncommon anionic entities. In particular, among the polytellurides, many motifs exist beyond the classical Q_n^{2-} chains (Q = S, Se, Te; $n = 1, 2, 3, ..., 13$). This includes infinite nonclassical motifs such as linear chains[1] or square-planar nets (with various distortions).[2−4] Two reviews summarized the large structural varieties of the polytellurides in 1988[5] and 2000,[6] including isolated motifs such as the bicyclic Te_8^{2-} with a four-bonded Te atom and the Te_5^{4-} anion with an almost linearly coordinated central Te atom, also found in Ba_2SnTe_5.[7] The central part of the latter anion, the (pseudo)linear triatomic unit, is the most simplistic example of a hypervalent molecule, isostructural and isoelectronic with the 22 valence-electron units XeF_2 and I_3^-, e.g., occurring in CsI_3[8] and $[Ph_4As]I_3$.[9] According to Rundle's hypervalency model,[10] such units are composed of three-center−four-electron (3c−4e) bonds, where the frontier orbital set is comprised of one filled σ-bonding molecular orbital (MO), one filled nonbonding MO, and one empty σ-antibonding MO.

An isolated linear hypervalent triatomic chalcogen anion was not known to exist, whereas several pnictides were published containing P_3^{7-}, As_3^{7-}, Sb_3^{7-}, and Bi_3^{7-}, namely, numerous examples of the $Ca_{14}AlSb_{11}$ type,[11] including the high-temperature thermoelectric $Yb_{14}MnSb_{11}$[12] as well as $Ca_{14-x}Eu_xMnSb_{11}$, exhibiting colossal magnetoresistance.[13] However, distorted Se_3 variants were observed in $Rb_{12}Nb_6Se_{35}$,[14] with Se−Se−Se bond angles of around 164°, presumably with the charge of 4−. Here we present the first example of a truly linear Se_3^{4-} anion of point group $D_{\infty h}$, occurring in the new silver selenide $Ba_2Ag_4Se_5$ and its Cu-substitution variants.

Experimental Section

Syntheses and Analyses. All reactions were commenced from the elements, which are always stored in an argon-filled glovebox. The elements were acquired in purities of at least 99%: barium

* To whom correspondence should be addressed. E-mail: kleinke@uwaterloo.ca.

(1) Schewe-Miller, I.; Böttcher, P. *J. Alloys Compd.* **1992**, *183*, 98−108.
(2) Patschke, R.; Kanatzidis, M. G. *Phys. Chem. Chem. Phys.* **2002**, *4*, 3266−3281.
(3) Malliakas, C.; Billinge, S. J. L.; Kim, H. J.; Kanatzidis, M. G. *J. Am. Chem. Soc.* **2005**, *127*, 6510−6511.
(4) Malliakas, C. D.; Kanatzidis, M. G. *J. Am. Chem. Soc.* **2006**, *128*, 12612−12613.
(5) Böttcher, P. *Angew. Chem., Int. Ed. Engl.* **1988**, *27*, 759−772.
(6) Smith, D. M.; Ibers, J. A. *Coord. Chem. Rev.* **2000**, *200−202*, 187−205.
(7) Assoud, A.; Derakhshan, S.; Soheilnia, N.; Kleinke, H. *Chem. Mater.* **2004**, *16*, 4193−4198.
(8) Tasman, H. A.; Boswijk, K. H. *Acta. Crystallogr.* **1955**, *8*, 59−60.
(9) Mooney Slater, R. C. L. *Acta. Crystallogr.* **1959**, *12*, 187−196.
(10) Rundle, R. E. *J. Am. Chem. Soc.* **1963**, *85*, 112−113.
(11) Cordier, G.; Schäfer, H.; Stelter, M. *Z. Anorg. Allg. Chem.* **1984**, *519*, 183−188.
(12) Brown, S. R.; Kauzlarich, S. M.; Gascoin, F.; Snyder, G. J. *Chem. Mater.* **2006**, *18*, 1873−1877.
(13) Kim, H.; Olmstead, M. M.; Klavins, P.; Webb, D. J.; Kauzlarich, S. M. *Chem. Mater.* **2002**, *14*, 3382−3390.
(14) Dürichen, P.; Bolte, M.; Bensch, W. *J. Solid State Chem.* **1998**, *140*, 97−102.

10.1021/ic701278b CCC: $37.00
Published on Web 10/04/2007

granules, 99%, from Aldrich; silver powder, −325 mesh, 99.9%, from Alfa Aesar; copper powder, −625 mesh, 99.9%, from Alfa Aesar, and selenium pellets, <4 mm, 99.99%, from Aldrich.

$Ba_2Ag_4Se_5$ was first encountered when trying to synthesize the hypothetical "$BaAg_4Se_3$", beginning with 1 mmol of Ba, 4 mmol of Ag, and 3 mmol of Se, and traces of I_2 as a mineralizer (99.99%, Alfa Aesar). This reaction mixture was put into a fused silica tube within the glovebox. The silica tube was sealed under dynamic vacuum of approximately 10^{-3} mbar. The evacuated tube was heated to 650 °C in a resistance furnace, held constant at this temperature for 12 h, and then cooled to 450 °C over a period of 1 week. Thereafter, the furnace was shut off, allowing the material to cool to room temperature. The reaction mixture was then ground and analyzed by means of X-ray powder diffraction (INEL diffractometer). Because no known material could be identified, the structure of the major phase was determined by single-crystal structure determination, described below, yielding the formula of $Ba_2Ag_4Se_5$.

Subsequently, phase pure $Ba_2Ag_4Se_5$ could be obtained by heating the elements in the stoichiometric ratio 2:4:5 to 700 °C, followed by annealing at 550 °C. Analogous sulfides or tellurides could not be prepared, and attempts to synthesize "$Ba_2Cu_4Se_5$" failed as well. However, almost half of the Ag atoms may be replaced with Cu atoms, up to $\delta = 1.8$ in $Ba_2Cu_\delta Ag_{4-\delta}Se_5$. This value was determined via single-crystal structure analysis from a crystal of a sample containing 50% Cu and 50% Ag, which included minor unidentified peaks in the X-ray powder diffractogram.

Energy-dispersive X-ray analysis (EDAX), using the electron microscope LEO 1530 with an additional EDAX device, EDAX Pegasus 1200, was performed to confirm the absence of any heteroelements, such as Si that might have come from the silica tube. The distribution of the elements Ba, Cu, Ag, and Se was homogeneous throughout the samples of $Ba_2Ag_4Se_5$ and $Ba_2CuAg_3Se_5$. For the latter, the Ba/Cu/Ag/Se ratio was determined to be 18:11:25:46 (in atom %), averaged over three crystals, which compares nicely with the nominal atom % ratio of 18:9:27:46.

Crystal Structure Determinations. Single-crystal data were obtained at room temperature with the Smart Apex CCD (Bruker) equipped with an area detector utilizing graphite-monochromated Mo Kα radiation. Three crystals were selected: one without any Cu, one from the reaction product of the nominal composition "$Ba_2CuAg_3Se_5$", and one from the reaction aiming at "$Ba_2Cu_2Ag_2Se_5$". In each case, two sets of 606 frames at different ϕ angles were measured with exposure times of 60 s each. The data were corrected for Lorentz and polarization effects. Absorption corrections were based on fitting a function to the empirical transmission surface as sampled by multiple equivalent measurements of numerous reflections.[15]

The ternary structure was determined first. Its unit cell dimensions indicated a centered monoclinic lattice. No systematic absences (besides those arising from the *C* centering) were observed, leaving *C*2, *Cm*, and *C*2/*m* as possible space groups. Structure solution and refinement using the *SHELXTL* package[16] were successful in the centrosymmetric space group *C*2/*m*. Because the refinements in the noncentrosymmetric space groups did not yield any substantial improvement, *C*2/*m* was chosen as the final space group. The structure solution via direct methods led to the identification of six sites, namely, one Ba, two Ag, and three Se sites. Subsequently, refining this model resulted in R1 = 0.0330; however, one Ag site, called Ag2, exhibited highly anisotropic displacement parameters, with $U_{33} \approx 5U_{22}$. Because no supercell reflections were observed, that site was refined as a split site, yielding a significantly lower *R* value of R1 = 0.0304 and two Ag2 sites, Ag2A and Ag2B, with occupancies of 64.2(9)% for Ag2A and 35.8% for Ag2B. The distance between these sites is 0.48 Å. Because no deficiencies were detected, the refined formula is $Ba_2Ag_4Se_5$.

Table 1. Crystallographic Data of $Ba_2Cu_\delta Ag_{4-\delta}Se_5$

refined formula	$Ba_2Ag_4Se_5$	$Ba_2Cu_{0.88(7)}Ag_{3.12}Se_5$	$Ba_2Cu_{1.78(7)}Ag_{2.22}Se_5$
fw [g mol^{-1}]	1100.96	1062.13	1022.27
T of measurement [K]	298(2)	298(2)	298(2)
wavelength [Å]	0.710 73	0.710 73	0.710 73
space group	*C*2/*m*	*C*2/*m*	*C*2/*m*
a [Å]	16.189(2)	16.101(2)	16.051(2)
b [Å]	4.5528(6)	4.4842(5)	4.4308(4)
c [Å]	9.2500(1)	9.208(1)	9.1480(9)
β [deg]	124.572(3)	124.101(2)	123.909(2)
V [Å^3]	561.4(1)	550.5(1)	539.93(9)
Z	2	2	2
ρ_{calcd} [g cm^{-3}]	6.513	6.408	6.288
R1 and wR2 (all data)[a]	0.0304, 0.0613	0.0411, 0.0857	0.0432, 0.0952
R1 and wR2 [$I > 2\sigma(I)$][a]	0.0277, 0.0601	0.0385, 0.0842	0.0405, 0.0933

[a] $R1 = \sum b||F_o| - |F_c||/\sum|F_o|$; $wR2 = [\sum[w(F_o^2 - F_c^2)^2]/\sum[w(F_o^2)^2]]^{1/2}$.

Table 2. Atomic Coordinates and Equivalent Displacement Parameters of $Ba_2Ag_4Se_5$

atom	site	*x*	*y*	*z*	U_{eq}[c]/Å^2	occ.
Ba	4i	0.31233(3)	0	0.31924(6)	0.0164(1)	1
Ag1[a]	4i	0.42379(6)	0	0.0447(1)	0.0319(2)	1
Ag2A[b]	4i	0.0624(2)	0	0.2442(6)	0.0356(7)	0.642(9)
Ag2B	4i	0.0591(4)	0	0.1888(9)	0.0356(7)	0.358
Se1	4i	0.12738(6)	0	0.8632(1)	0.0181(2)	1
Se2	4i	0.65681(6)	0	0.2966(1)	0.0157(2)	1
Se3	2c	0	0	$^1/_2$	0.0221(3)	1

[a] $Ba_2Cu_{0.88}Ag_{3.12}Se_5$: 0.81(2) Ag, 0.19 Cu. $Ba_2Cu_{1.78}Ag_{2.22}Se_5$: 0.58(2) Ag, 0.42 Cu. [b] $Ba_2Cu_{0.88}Ag_{3.12}Se_5$: 0.75(2) Ag, 0.25 Cu. $Ba_2Cu_{1.78}Ag_{2.22}Se_5$: 0.53(2) Ag, 0.47 Cu. [c] U_{eq} is defined as one-third of the trace of the orthogonalized U_{ij} tensor.

Next, we refined the two data sets containing both Cu and Ag, commencing from the sites obtained for $Ba_2Ag_4Se_5$ (without splitting the Ag2 site). Thereby, we allowed for Cu/Ag mixing on both Ag sites and found that both sites accommodate Cu in both cases. The formulas were refined to $Ba_2Cu_{0.88(7)}Ag_{3.12}Se_5$ and $Ba_2Cu_{1.78(7)}Ag_{2.22}Se_5$, respectively. The formula $Ba_2Cu_{0.88(7)}Ag_{3.12}Se_5$ is within 2 standard deviations equivalent to the nominal composition of $Ba_2CuAg_3Se_5$, while $Ba_2Cu_{1.78(7)}Ag_{2.22}Se_5$ contains significantly less Cu than the starting composition "$Ba_2Cu_2Ag_2Se_5$", indicating that the phase range of $Ba_2Cu_\delta Ag_{4-\delta}Se_5$ does not reach $\delta = 2$. Crystallographic details are given in Table 1, and atomic positions, displacement, and occupancy factors are given in Table 2.

Electronic Structure Calculations. To model the structure of $Ba_2Ag_4Se_5$, we initially used the averaged Ag2 site. Two more models were calculated based on the final refinements: one thereof using the Ag2A site and the other with exclusively the Ag2B site filled. Moreover, commencing from the refinement of $Ba_2Cu_{1.78(7)}Ag_{2.22}Se_5$, the electronic structure of $Ba_2Cu_2Ag_2Te_5$ was modeled by filling one of the two Ag1 and Ag2 sites with Cu, resulting in a symmetry reduction to *Cm*.

The computations were performed by employing the self-consistent tight-binding *first principles* LMTO method (LMTO = linear muffin tin orbitals) with the atomic spheres approximation.[17,18] In the LMTO approach, the density functional theory (DFT) is

(15) *SAINT*, version 4; Siemens Analytical X-ray Instruments Inc.: Madison, WI, 1995.
(16) Sheldrick, G. M. *SHELXTL*, version 5.12; Siemens Analytical X-ray Systems: Madison, WI, 1995.

employed utilizing the local density approximation for the exchange correlation energy.[19] The following wavefunctions were used: for Ba, 6s, 5d, 4f, and 6p included via the downfolding technique;[20] for Ag, 5s, 5p, 4d, and 4f (downfolded); for Cu, 4s, 4p, and 3d; and for Se, 4s, 4p, and 3d (the latter two were downfolded). The 242 independent *k* points of the first Brillouin zone were chosen via an improved tetrahedron method.[21] To analyze the extent of the Ag−Ag and Se−Se interactions, selected integrated COHP values (ICOHPs; COHP = crystal orbital Hamilton populations)[22,23] were calculated as well.

Finally, the MO diagram of the linear Se_3^{4-} unit of $Ba_2Ag_4Se_5$ was calculated using Gaussian,[24] employing the B3LYP method with the 3-21G basis set.[25]

Electrical Conductivity Measurement. The phase-pure sample of $Ba_2CuAg_3Se_5$ was pressed into a bar-shaped pellet of dimensions $6 \times 1 \times 1$ mm^3 because no single crystals of sufficient dimensions were available. The achieved density was about 80% of the theoretical maximum as determined by the single-crystal structure study. The specific electrical conductivity, σ, of this pellet was determined by using a four-point-method, where the contacts were made with silver paint (TED PELLA): a homemade device was used to determine the voltage drops ΔV under dynamic vacuum between 320 and 200 K. The resistances (R) were calculated from the voltage drops using Ohm's law, i.e., $R = \Delta V/I$, with I = current. We calculated σ(T) after measuring the lengths between the contacts, L, according to $\sigma = L/AR$, with the area $A = 1 \times 1$ mm^2.

Results and Discussion

Crystal Structure. The isostructural series $Ba_2Cu_\delta Ag_{4-\delta}Se_5$ ($0 < \delta < 1.8$) forms a new layered structure type shown in Figure 1 for $Ba_2Ag_4Se_5$. Covalent Ag−Se layers alternate along the *a* axis with puckered sheets of Ba atoms that are eightfold-coordinated by Se atoms in the form of distorted square antiprisms.

The Ba−Se distances vary between 3.29 and 3.53 Å in $Ba_2Ag_4Se_5$ (Table 3). Related Ba−Se square antiprisms were found in $BaAg_2SnSe_4$ (3.41−3.43 Å) and $BaCu_2SnSe_4$ (3.33−3.42 Å),[26] but lower and higher coordination numbers ranging from six to nine for barium selenides are known as well.[27,28] Replacing part of the Ag atoms with Cu leads to a continuous albeit anisotropic decrease of all lattice parameters because of the smaller size of Cu: the Pauling radii are 1.34 Å for Ag and 1.18 Å for Cu. Hence, the Ag/Cu−Se distances shrink significantly, causing a unit cell contraction and thereby minor changes to the Ba−Se bonds as well. For example, for $Ba_2Cu_{1.8}Ag_{2.2}Se_5$, the Ba−Se bonds range from 3.29 to 3.49 Å, averaging 3.335 Å compared to 3.350 Å in $Ba_2Ag_4Se_5$.

The Ag−Se layer of $Ba_2Ag_4Se_5$ is comprised of $[Ag_4Se_5]^{4-}$ chains extending along the *b* axis (Figure 2), which are interconnected to layers by the Se_3 units along the *c* axis. The connection stems from Ag atoms of two chains both being bonded to the same central Se atom of the Se_3 unit. The Se coordination of the Ag atoms is best described as [3

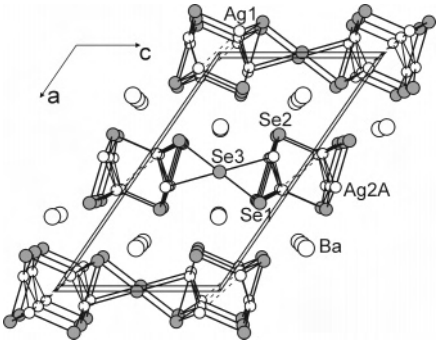

Figure 1. Crystal structure of $Ba_2Ag_4Se_5$ (excluding the Ag2B site): large white circles, Ba; small white circles, Ag; gray circles, Se. Ba−Se bonds are omitted for clarity.

Table 3. Selected Interatomic Distances [Å] of $Ba_2Cu_\delta Ag_{4-\delta}Se_5$[a]

		$Ba_2Ag_4Se_5$	$Ba_2Cu_{0.88(7)}Ag_{3.12}Se_5$	$Ba_2Cu_{1.78(7)}Ag_{2.22}Se_5$
Ba−Se1	2×	3.2941(7)	3.286(1)	3.290(1)
Ba−Se1		3.525(1)	3.520(1)	3.493(1)
Ba−Se2		3.296(1)	3.290(1)	3.293(1)
Ba−Se2	2×	3.3115(7)	3.303(1)	3.299(1)
Ba−Se3	2×	3.3828(5)	3.3692(5)	3.3574(5)
M1−Se1	2×	2.7196(6)	2.679(1)	2.637(1)
M1−Se2		2.644(1)	2.605(2)	2.558(2)
M1−Se2		3.055(2)	3.066(2)	3.008(2)
M1−M1		3.014(2)	2.954(3)	2.895(3)
M1−M2	2×	2.987(2)	2.933(1)	2.903(1)
M2−Se1		2.639(3)	2.610(2)	2.552(2)
M2−Se2	2×	2.629(2)	2.5732(9)	2.535(1)
M2−Se3		3.054(5)	3.130(2)	3.096(2)
M2−M1	2×	2.987(2)	2.933(1)	2.903(1)
Se1−Se3		2.7706(9)	2.783(1)	2.783(1)
Se3−Se1	2×	2.7706(9)	2.783(1)	2.783(1)
Ag2B−Se1		2.775(6)		
Ag2B−Se2	2×	2.624(3)		
Ag2B−Se3		3.511(6)		
Ag2B−Ag1	2×	2.906(4)		
Ag2B−Ag1	2×	3.255(5)		
Ag2B−Ag2A		3.312(6)		
Ag2B−Ag2B		2.88(1)		

[a] M1: Ag1 in $Ba_2Ag_4Se_5$, Ag1/Cu1 mixed occupied in the quaternary selenides. M2: Ag2A in $Ba_2Ag_4Se_5$, Ag2/Cu2 mixed occupied in the quaternary selenides.

(17) Andersen, O. K. *Phys. Rev. B* **1975**, *12*, 3060−3083.
(18) Skriver, H. L. *The LMTO Method*; Springer: Berlin, Germany, 1984.
(19) Hedin, L.; Lundqvist, B. I. *J. Phys. C* **1971**, *4*, 2064−2083.
(20) Lambrecht, W. R. L.; Andersen, O. K. *Phys. Rev. B* **1986**, *34*, 2439−2449.
(21) Blöchl, P. E.; Jepsen, O.; Andersen, O. K. *Phys. Rev. B* **1994**, *49*, 16223−16233.
(22) Dronskowski, R.; Blöchl, P. E. *J. Phys. Chem.* **1993**, *97*, 8617−8624.
(23) Landrum, G. A.; Dronskowski, R. *Angew. Chem., Int. Ed.* **2000**, *39*, 1560−1585.
(24) Frisch, M. J.; Trucks, G. W.; Schlegel, H. B.; Scuseria, G. E.; Robb, M. A.; Cheeseman, J. R.; Zakrzewski, V. G.; Montgomery, J. A.; Stratmann, R. E.; Burant, J. C.; Dapprich, S.; Millam, J. M.; Daniels, A. D.; Kudin, K. N.; Strain, M. C.; Farkas, O.; Tomasi, J.; Barone, V.; Cossi, M.; Cammi, R.; Mennucci, B.; Pomelli, C.; Adamo, C.; Clifford, S.; Ochterski, J.; Petersson, G. A.; Ayala, P. Y.; Cui, Q.; Morokuma, K.; Malick, D. K.; Rabuck, A. D.; Raghavachari, K.; Foresman, J. B.; Cioslowski, J.; Ortiz, J. V.; Baboul, A. G.; Stefanov, B. B.; Liu, G.; Liashenko, A.; Piskorz, P.; Komaromi, I.; Gomperts, R.; Martin, R. L.; Fox, D. J.; Keith, T.; Al-Laham, M. A.; Peng, C. Y.; Nanayakkara, A.; Gonzalez, C.; Challacombe, M.; Gill, P. M. W.; Johnson, B.; Chen, W.; Wong, M. W.; Andres, J. L.; Gonzalez, C.; Head-Gordon, M.; Replogle, E. S.; Pople, J. A. *Gaussian 98*, revision A.7; Gaussian, Inc.: Pittsburgh, PA, 1998.
(25) Pietro, W. J.; Francl, M. M.; Hehre, W. J.; DeFrees, D. J.; Pople, J. A.; Binkley, J. S. *J. Am. Chem. Soc.* **1982**, *104*, 5039−5048.
(26) Assoud, A.; Soheilnia, N.; Kleinke, H. *Chem. Mater.* **2005**, *17*, 2255−2261.
(27) Assoud, A.; Soheilnia, N.; Kleinke, H. *Chem. Mater.* **2005**, *17*, 4509−4513.
(28) Assoud, A.; Soheilnia, N.; Kleinke, H. *J. Solid State Chem.* **2005**, *178*, 1087−1093.

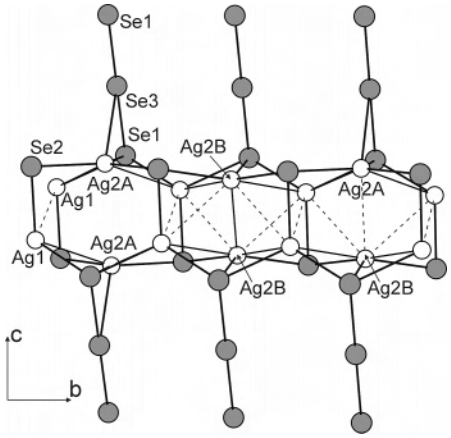

Figure 2. $[Ag_4Se_5]^{4-}$ chain of $Ba_2Ag_4Se_5$ running along [010]. Either the Ag2A or Ag2B atom is present at a given site. Code: white circles, Ag; gray circles, Se.

+ 1]: Ag1 has three Se neighbors at distances between 2.64 and 2.72 Å and a fourth Se atom at a distance of 3.06 Å, while three Ag2A−Se distances are between 2.63 and 2.64 Å, with a fourth at 3.05 Å. More extreme than the other sites, the Ag2B site boasts a fourth Ag2B−Se distance as long as 3.51 Å.

The refinements of the quaternary selenides show that the Cu atoms exhibit a slight preference toward the Ag2 site, most likely because of the shorter Ag2−Se distances. For example, in $Ba_2Cu_{1.8}Ag_{2.2}Se_5$, the former Ag1 site accommodates 42% Cu, compared to 47% Cu on the former Ag2 site (Table 2). Therein, the M1 site forms three bonds with Se atoms between 2.56 and 2.64 Å, and the M2 site forms three bonds ranging from 2.54 to 2.55 Å.

The highly anisotropic Se coordination of the Ag atoms is caused by intermediate Ag−Ag contacts. Ag1 participates in three Ag−Ag bonds (2.99−3.01 Å) and Ag2A in two (both 2.99 Å). The Ag2B site, refined to be occupied by 36% in $Ba_2Ag_4Se_5$, is shifted toward the neighboring Ag2 site, as well as toward Ag1, resulting in a shortened Ag2B−Ag2B bond of 2.88 Å and two Ag2B−Ag1 bonds of 2.91 Å. These bonds are comparable to the bond in elemental Ag (2.89 Å).

Three repeated units of the $[Ag_4Se_5]^{4-}$ chain are displayed in Figure 2, with two Ag2 sites per cell related by the twofold rotation axis running along the *b* axis. Per repeat unit, three different Ag2A/Ag2B combinations are possible, namely, two Ag2A (shown in the left part of Figure 2), two Ag2B (central part), and one Ag2A and one Ag2B (right part). This results in three different Ag−Ag distances between these sites, namely, the long Ag2A−Ag2A distance of 3.76 Å, the intermediate Ag2A−Ag2B distance of 3.31 Å, and the short Ag2B−Ag2B distance of 2.88 Å. For comparison, the shortest Ag−Ag interaction of $Ba_2AgSnSe_4$ is 3.21 Å and was calculated to exhibit significant bonding character with an ICOHP value of −0.24 eV.[26] Ag−Ag (as well as Cu−Cu) bonds are not uncommon in such chalcogenides, although the coinage group metals are typically in their 1+ state, hence, formally closed-shell (d^{10}). These interactions are thought to be bonding due to the hybridization with the energetically higher lying s and p orbitals.[29−31]

On the basis of the formation of shorter Ag−Ag interactions involving Ag2B, one may postulate that the driving force for the Ag2 split site is the formation of stronger Ag−Ag bonding at the expense of the Ag−Se interactions (in addition to the gain in configurational entropy). Figure 2 also clarifies that Ag ion conductivity is highly unlikely to occur, for the Ag ions could only propagate along the *b* axis, which is the chain direction. Along the *b* axis, the Ag2 atoms would have to move past the fully occupied Ag1 sites, inhibiting ionic conductivity.

A unique feature of the $Ba_2Ag_4Se_5$ structure is its linear Se_3 unit. The classical Zintl anions Se_3^{2-} with 20 valence electrons are bent with bond angles between 102° and 112° and Se−Se single bonds of 2.4 Å. Examples of the bent units include the alkali-metal selenides $(A^+)_2Se_3^{2-}$, where the assignment of charges is unambiguous, e.g., K_2Se_3 (bond angle 102.6°; bond length 2.38 Å),[32] Rb_2Se_3 (103.5°; 2.38 Å), and Cs_2Se_3 (103.5°; 2.35 Å).[33] These bonds compare well with the doubled Se radius; e.g., after Pauling, $2r_{Se} = 2.34$ Å.[34] Isoelectronic and topologically equivalent bent Se_3^{2-} units were also found in ternary alkaline-earth selenides, specifically in Sr_2SnSe_5 (bond angle 107.9°; bond length 2.39 Å)[35] and Ba_2SnSe_5 (bond angles 108.3−110.6°; bond lengths 2.38−2.44 Å).[28] While a linear Se_3 unit was not previously discovered, two Se_3 units of the ternary selenide $Rb_{12}Nb_6Se_{35}$[14] exhibit bond angles of 163° and 164°, with significantly longer Se−Se interactions of 2.59−2.64 Å. Moreover, related Se_3 fragments occur within Se_4 and Se_5 units with Se−Se−Se angles of 166° and 143° in $K_3CuNb_2Se_{12}$[36] and Nb_2Se_9,[37] respectively. The Se_3 unit of $Ba_2Ag_4Se_5$ is truly linear, point group $D_{\infty h}$, displaying a bond angle of 180°, with Se−Se bonds of 2.77 Å. This bond distance remains almost unchanged upon Cu substitution, reaching 2.78 Å in the case of $Ba_2Cu_{1.8}Ag_{2.2}Se_5$.

Noting that the Se2 atom of $Ba_2Ag_4Se_5$ does not participate in any Se−Se interactions, we assign the formal charges according to $(Ba^{2+})_2(Ag^+)_4Se_3^{4-}(Se^{2-})_2$ and hence obtain $3 \times 6 + 4 = 22$ valence electrons for the Se_3^{4-} unit. Thus, the linear Se_3^{4-} unit is isoelectronic with XeF_2, the linear polyantimonide Sb_3^{7-} found in $Ca_{14}AlSb_{11}$[38] and the more common polyiodide I_3^-, e.g., found in CsI_3[8] and $[Ph_4As]I_3$.[9] A simplifying MO approach, already discussed back in 1963,[10] encompasses only three p orbitals of XeF_2 that lie on the F−Xe−F axis, e.g., the p_z orbitals, considering the s orbitals and the other p orbitals as lone pairs. The resulting MO diagram then comprises three MOs. Two of them are

(29) Mehrotra, P. K.; Hoffmann, R. *Inorg. Chem.* **1978**, *17*, 2187−2189.
(30) Merz, K. M.; Hoffmann, R., Jr. *Inorg. Chem.* **1988**, *27*, 2120−2127.
(31) Pyykkö, P. *Chem. Rev.* **1997**, *97*, 597−636.
(32) Böttcher, P. *Z. Anorg. Allg. Chem.* **1977**, *432*, 167−172.
(33) Böttcher, P. *Z. Anorg. Allg. Chem.* **1980**, *461*, 13−21.
(34) Pauling, L. *The Nature of the Chemical Bond*, 3rd ed.; Cornell University Press: Ithaca, NY, 1948.
(35) Assoud, A.; Soheilnia, N.; Kleinke, H. *Chem. Mater.* **2004**, *16*, 2215−2221.
(36) Lu, Y.; Ibers, J. A. *Inorg. Chem.* **1991**, *30*, 3317−3320.
(37) Sunshine, S. A.; Ibers, J. A. *Acta. Crystallogr. C* **1987**, *43*, 1019−1022.
(38) Cordier, G.; Schäfer, H.; Stelter, M. *Z. Anorg. Allg. Chem.* **1984**, *519*, 183−188.

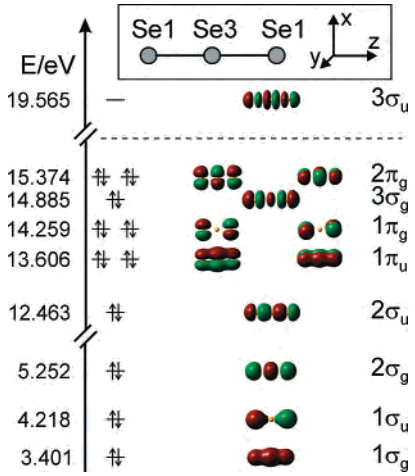

Figure 3. MO diagram of the linear Se_3^{4-} unit.

filled, σ-bonding and nonbonding MOs, while the σ-antibonding MO remains empty.

Munzarova and Hoffmann's recent review supports the validity of this model.[39] The resulting bonding situation may be described as a 3c−4e bond, a so-called "half-bond", validating the observation of elongated distances, compared to the classical single bonds. For example, the linear Sb_3^{7-} unit in $Ca_{14}AlSb_{11}$ exhibits two Sb−Sb distances of 3.20 Å, compared to Sb−Sb single bonds of 2.80−2.85 Å, and linear I_3^- in $[Ph_4As]I_3$ comprises two I−I distances of 2.9 Å, significantly longer than the single bond in I_2 of 2.76 Å.[40] The elongation of the Se−Se distances in $Ba_2Ag_4Se_5$ is comparable, with its 2.77 Å vs the 2.34 Å for the Se−Se single bond.

The MO diagram computed for the Se_3^{4-} unit of $Ba_2Ag_4Se_5$ (Figure 3) confirms the postulated fractional bond order. The lowest three valence orbitals have predominantly 4s character and are σ-bonding ($1\sigma_g$), nonbonding ($1\sigma_u$), and σ-antibonding ($2\sigma_g$). All six π MOs originating from the p_x and p_y orbitals are filled, namely, the two bonding $1\pi_u$ MOs, the two nonbonding $1\pi_g$ MOs, and the two antibonding $2\pi_g$ MOs. The s−p mixing is significant, with Se being a row 4 element, causing the nodal plane at the central atom of the $3\sigma_g$ MO of Rundle's model (formed by the p_z orbitals) to disappear, which, in turn, is reflected in antibonding character and hence a shift above the nonbonding $1\pi_g$ MOs. A gap of almost 4.2 eV separates the highest occupied molecular orbital, the two degenerated $2\pi_g$ MOs, from the lowest unoccupied molecular orbital, the $3\sigma_u$ MO. Hence, the only unfilled MO, principally composed of the antibonding combination of the p_z orbitals, is of σ-antibonding character, while the π orbitals may be treated as lone pairs.[39] Therefore, the DFT-based MO calculation also results in σ-bonding 3c−4e interactions.

Electronic Structure. The counting scheme of $(Ba^{2+})_2(Ag^+)_4Se_3^{4-}(Se^{2-})_2$ mentioned above indicates an electron-precise compound, with the 4d orbitals of Ag filled, as well as all Se states except for the $3\sigma_g$ MO of the Se_3 unit. The band structure calculation of the averaged $Ba_2Ag_4Se_5$ model reveals a direct band gap of 0.9 eV separating the valence band from the conduction band, whose bottom is predominated by the p_z states of the Se_3 unit, as emphasized via the *fat-band* representation (Figure 4).[41] Similar band gaps were obtained from the calculations using exclusively the Ag2A site (1.0 eV) and the Ag2B site (0.8 eV). Moreover, the model for $Ba_2Cu_2Ag_2Se_5$ showed comparable densities of states, with a band gap of 1.0 eV.

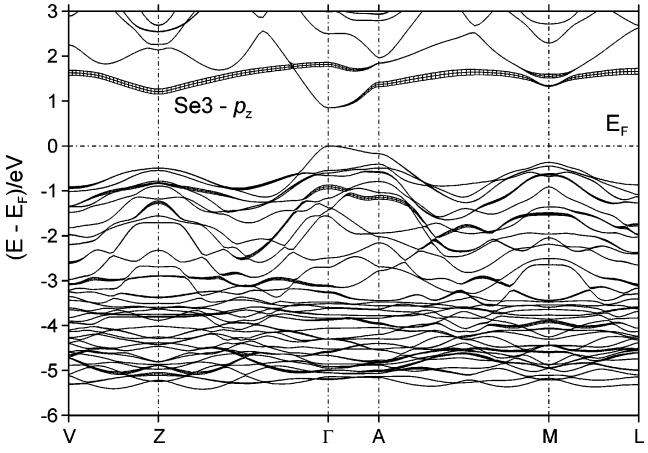

Figure 4. Band structure of $Ba_2Ag_4Se_5$, highlighting the Se3 p_z contributions. The Fermi level, E_F, was arbitrarily placed at 0 eV.

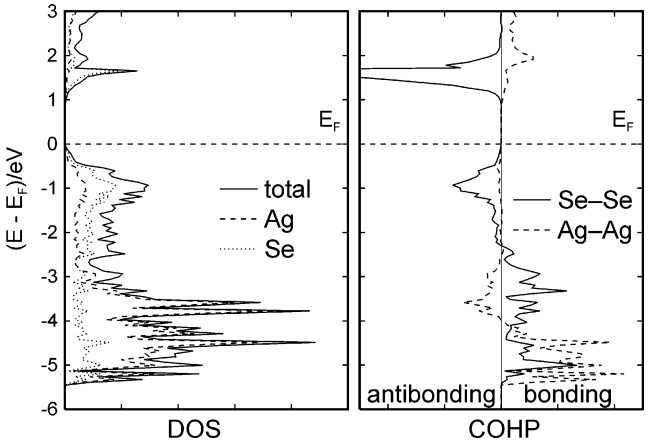

Figure 5. Densities of states (DOS, left) and selected crystal orbital Hamilton population curves (COHP, right) of $Ba_2Ag_4Se_5$. The Fermi level, E_F, was arbitrarily placed at 0 eV.

As shown in the atomic projections of the densities of states (left part of Figure 5), the top of the valence band is mostly comprised of the filled Se p states, while the Ag d states are located toward the bottom, between −3 and −5.5 eV. The Ag−Ag COHP curves (right part of Figure 5), cumulated over all interactions <3.2 Å per cell, are net bonding, although antibonding states start to become filled at −4 eV. The Se−Se bond of 2.77 Å of the Se_3 unit also exhibits filled antibonding states, commencing at −2 eV, which resemble the Gaussian calculation of the isolated Se_3^{4-} unit. The gap between bonding and antibonding Se−Se states of 0.9 eV is much smaller in the solid because of the mixing with the Ag states. The ICOHP value of the 2.77 Å Se−Se

(39) Munzarova, M. L.; Hoffmann, R. *J. Am. Chem. Soc.* **2002**, *124*, 4787−4795.
(40) Mooney, R. C. *Acta Crystallogr.* **1959**, *12*, 187.
(41) Jepsen, O.; Andersen, O. K. *Z. Phys.* **1995**, *97*, 25.

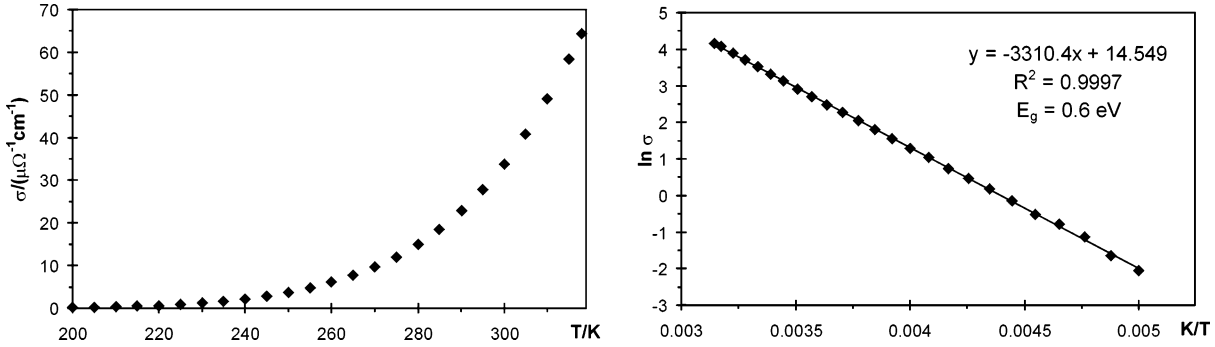

Figure 6. Electrical conductivity of $Ba_2CuAg_3Se_5$.

bond of −1.07 eV indicates a net bonding character, as was predicted by the MO calculation.

The Ag2B site differs from the Ag2A site considering its shorter Ag−Ag and longer Ag−Se interactions. The ICOHP calculations of the Ag−Ag bonds reveal a strong bond length/bond strength correlation; e.g., the shortest bond, the Ag2B−Ag2B bond of 2.88 Å, is the strongest one with an ICOHP = −0.71 eV. In contrast, the corresponding Ag2A−Ag2A distance of 3.76 Å is nonbonding (ICOHP = +0.004 eV), as is the Ag1−Ag2A distance of 3.61 Å (−0.01 eV), while the Ag1−Ag2B interaction of 3.26 Å is significantly bonding (−0.29 eV). On the other hand, the long Ag2A−Se3 interaction of 3.05 Å is bonding with an ICOHP = −0.25 eV, whereas the corresponding Ag2B−Se3 distance of 3.51 Å is basically nonbonding with an ICOHP = −0.02 eV. Hence, it can be concluded that the driving force of the split site is the formation of stronger Ag−Ag bonding, at the expense of Ag−Se bonding.

Physical Properties. The electronic structure calculations were indicative of semiconducting character for $Ba_2Cu_\delta Ag_{4-\delta}Se_5$, with band gaps between 0.8 and 1.0 eV depending on the model. Correspondingly, the electrical conductivity of the pellet of $Ba_2CuAg_3Se_5$ is very low and increases exponentially with increasing temperature, reaching 30 $\mu\Omega^{-1}$ cm^{-1} at room temperature (left part of Figure 6). The exponential increase is typical for an intrinsic semiconductor and enables us to calculate the activation energy from the slope of the ln σ vs $1/T$ diagram shown in the right part of Figure 6 via Arrhenius' law for thermally activated conduction: $\ln \sigma/\sigma_0 = \exp(-\Delta_A/k_BT)$, with Δ_A = activation energy. The linear fit was computed to have a regression coefficient of $R^2 = 0.9997$. With its slope being $-\Delta_A/k_B$ and $E_{gap} = 2\Delta_A$,[42] the experimental band gap was calculated to be 0.6 eV.

The low value of the electrical conductivity is, in part, a consequence of using a cold-pressed pellet with a density of 80%. For example, hot pressing a powderized sample of $Re_3Ge_{0.6}As_{6.4}$ increased the conductivity of the cold-pressed pellet from 60 to 1090 Ω^{-1} cm^{-1}, i.e., by a factor of almost 20.[43] It is also noted that $Ba_2Cu_\delta Ag_{4-\delta}Se_5$ is a layered material, where Ba^{2+} cations connect the covalent Cu/Ag−Se layers along the crystallographic *a* axis. The anisotropic character of the electrical conductivity can hence be expected, with the smallest conductivity values found along the *a* axis, but measurement of the pellet cannot reveal this.

Conclusions

A new selenide, $Ba_2Ag_4Se_5$, together with its Cu variants $Ba_2Cu_\delta Ag_{4-\delta}Se_5$ ($\delta < 2$), was prepared, its crystal structure was solved, and its physical properties were calculated and experimentally determined. In this new structure type, Ba layers alternate with Cu/Ag−Se layers, which, in turn, are composed of chains interconnected by unique Se_3 units. These units are the first linear Se_3^{4-} anions, isoelectronic with XeF_2 and I_3^-. Supported by our Gaussian calculation, the Se−Se bonds thereof are described best as 3c−4e bonds, in accordance with their elongation with respect to Se−Se single bonds. The characterization of $Ba_2Ag_4Se_5$ as a semiconductor supports the assignment of four negative charges to the Se_3 fragments in $(Ba^{2+})_2(Ag^+)_4Se_3^{4-}(Se^{2-})_2$.

Acknowledgment. Financial support from NSERC, CFI, OIT (Ontario Distinguished Researcher Award for H.K.), the Province of Ontario (Premier's Research Excellence Award for H.K.), and the Canada Research Chair program (CRC for H.K.) is greatly appreciated.

Supporting Information Available: Three X-ray crystallographic files (CIF) and a figure displaying the thermal expansion parameters of the Ag2 split sites. This material is available free of charge via the Internet at http://pubs.acs.org.

IC701278B

(42) Kittel, C. *Introduction to Solid State Physics*, 7th ed.; John Wiley & Sons, Inc.: New York, 1996.

(43) Soheilnia, N.; Xu, H.; Zhang, H.; Tritt, T. M.; Swainson, I.; Kleinke, H. *Chem. Mater.* **2007**, *19*, 4063−4068.